CdTe quantum dots-encapsulated ZnO nanorods for high-efficient photoelectrochemical degradation of phenols

Danqing Liu,[a,c] Zhaozhu Zheng,[a] Chaoqun Wang,[c] Yongqi Yin,[b] Shaoqin Liu,[a*] Bin Yang,[b*] Zhaohua Jiang[c*]

[a] Key Laboratory of Microsystems and Microstructures Manufacturing (Harbin Institute of Technology), Ministry of Education, Harbin 150080, China

[b] Condensed Matter Science and Technology Institute, Harbin Institute of Technology, Harbin 150080, China

[c] School of Chemical engineering, Harbin Institute of Technology, Harbin 150080, China

[*]Corresponding author: shaoqinliu@hit.edu.cn (S. Q. L.), binyang@hit.edu.cn (B. Y.), jiangzhaohua@hit.edu.cn (Z. H. J.)

Experimental section

Synthesis of tris-l,10-phenanthroline complexes of cobalt(II), [Co(Phen)$_3$]Cl$_2$.

Tris-l, 10-phenanthroline complexes of cobalt(II), [Co(Phen)$_3$]Cl$_2$, was prepared by mixing CoCl$_2$ and l,10-phenanthroline (Phen) in a 1:3 molar ratio.

Synthesis of MPA-capped CdTe QDs. The MPA-capped CdTe QDs were prepared according to a previously published procedure from our laboratory.[S1] 0.986 g of Cd(ClO$_4$)$_2$·6H$_2$O was dissolved in 125 mL of distilled water, and then 0.43 mL of MPA was added. The pH value was adjusted to 11.2 by adding 2 M NaOH. The solution was placed in a three-neck flask and deaerated by N$_2$ gas for about 30 min. H$_2$Te gas generated by the mixture of 0.2 g of Al$_2$Te$_3$ and 15 mL of 0.5 M H$_2$SO$_4$ in another three-neck flask was directed into the prepared solution. The mixture was then refluxed at 105 ºC for 48 h in N$_2$ gas. The absorbance shoulder of MPA-capped CdTe QDs was located at 545 nm, while the photoluminescence peak of QDs was situated at 595 nm (Fig. S1). The size and concentration of CdTe QDs in the solution were estimated from the UV-Vis spectrum to be around 3.24 nm and 6.99 × 10^{-5} M, respectively, according to the Peng's empirical equation.[S2]
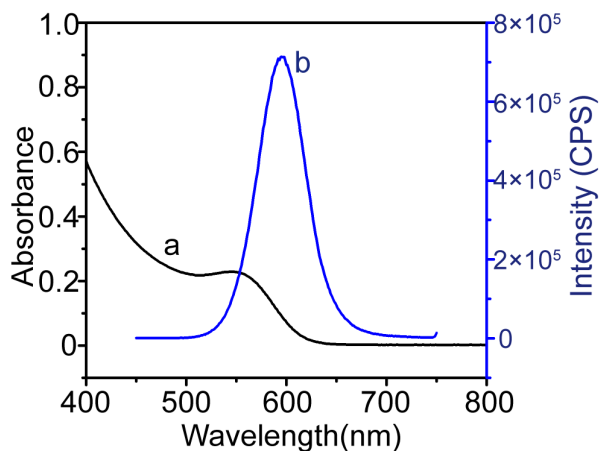

Figure S1. UV-Vis (black curve, a) and luminescence spectra (blue curve, b) of MPA-capped CdTe QDs in solution.

Determination of phenol concentration. The concentration of phenol was determined based on the Emerson's method.[S3] At each checkpoint, 500 μL of solution from the reactor was added to a 25 mL volumetric flask. Then, 500 μL of

4-aminoantipyrine solution (2%), 500 µL of potassium ferricyanide (8%) and 250 µL of ammonia were added to the volumetric flask and diluted with deionized water to volume and mixed. The volumetric flask was incubated in the dark for 10 min. The absorbance at 510 nm was recorded.

Identification of the reaction intermediates. The reaction intermediates were analyzed by gas chromatography coupled with mass spectrometry (GC-MS, Agilent 7890A and 5975C, Agilent Tech.) using a 30 cm HP-5 column (Hewlett-Packard). In order to detect the intermediate products, GC-MS measurements were performed as follows. After reactions were stopped, the solution (15mL) was dried by freezing-drying. The resulting material was dissolved by diethyl ether and precipitate was separated by centrifugation. The pellucid solution was dried and derivatized by 50 µL MSTFA and 0.5 µL TMIS at 62 °C for 70 min.[S4] Then 1 µL was analyzed on the GC-MS. GC-MS analyses were carried out on a GC ultra gas chromatograph (7890A, Agilent Technologies) using a 30 cm HP-5 column, coupled with a mass spectrometer (5975C, Agilent Technologies). The injector port was set for split operation at 280 °C. The temperature program of the column was as follows: at 50 °C, hold time = 2 min; from 50 to 150 °C, rate = 30 °C/min. Because the background produced by derivatization was complex, 15 mL 0.07 M Na_2SO_4 solution was used to do the blank test using the same method.

Part 1 Preparation and characterization of CdTe QD encapsulated ZnO nanorod arrays.
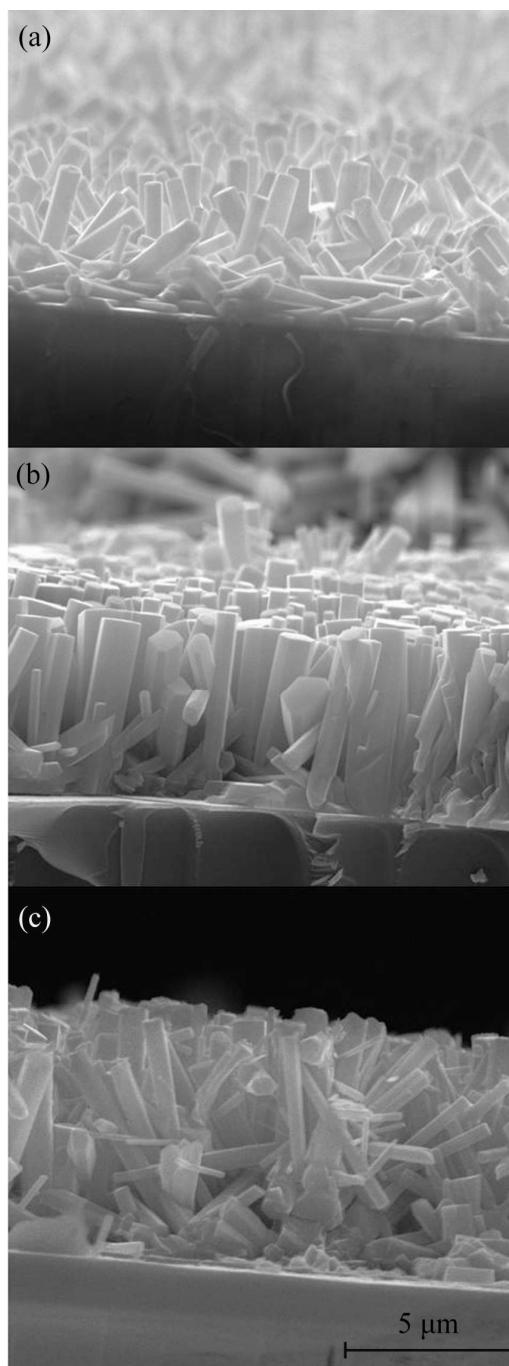

Figure S2. SEM images of ZnO nanorod arrays with different growth times: (a) 5 h, (b) 10 h, and (c) 15 h. The length of these nanorods is 3.4, 5.2 and 8.1 μm when the reaction time is 5, 10 and 15 h, respectively.
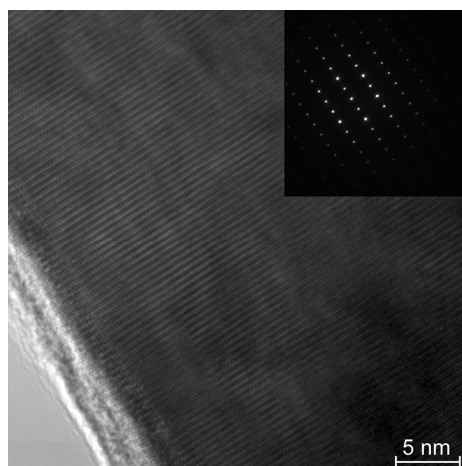
Figure S3. HRTEM image and corresponding diffraction pattern (inset) of ZnO nanorod arrays fabricated on ITO substrates by a hydrothermal method with pH 8.4 at 90 ºC for 2.5 h, which exhibits the single crystalline structure with the [0001] growth direction.
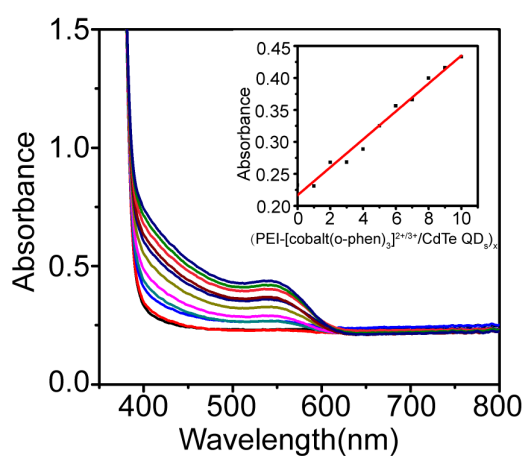

Figure S4. UV-Vis spectra of growing (PEI-[cobalt(o-phen)$_3$]$^{2+/3+}$/CdTe QD)$_x$ multilayers (from bottom to up: x = 0-10). Inset shows a plot of 550 nm versus the number of bilayers, x. Regular layer growth is revealed by a linear dependence of the absorbance determined at 550 nm versus x, and the absorbance increase for one bilayer of PEI-[cobalt(o-phen)$_3$]$^{2+/3+}$/CdTe QDs at 550 nm is 0.021 ± 0.0003.
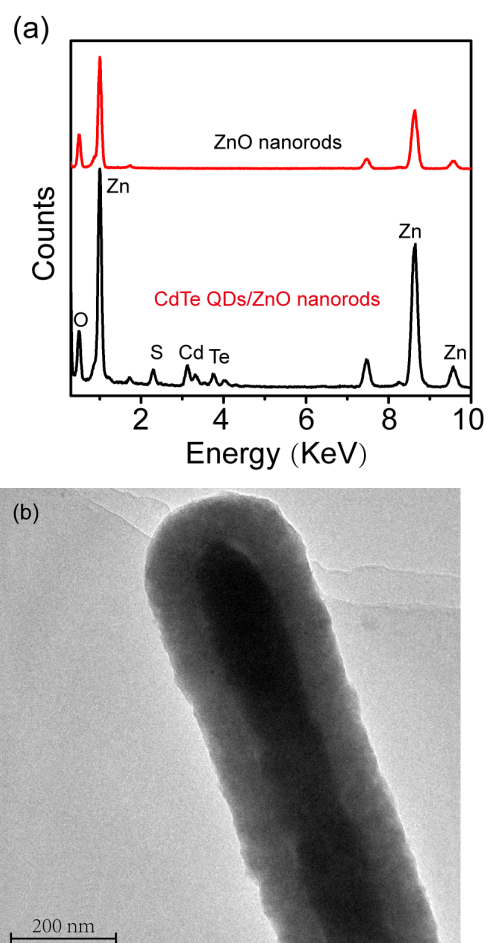
Figure S5. (a) EDX spectra of ZnO nanorod arrays and 20 bilayers of [cobalt(o-phen)$_3$]$^{2+/3+}$-PEI/CdTe QD encapsulated ZnO nanorod arrays. (b) TEM image of 20 bilayers of [cobalt(o-phen)$_3$]$^{2+/3+}$-PEI/CdTe QD encapsulated ZnO nanorod arrays.
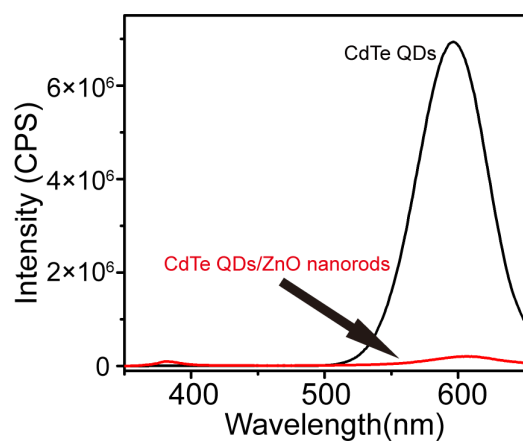
Figure S6. Luminescence spectra of MPA-capped CdTe QDs in solution (black curve) and ZnO nanorods grown on the ITO electrode after coated with 20 [cobalt(o-phen)$_3$]$^{2+/3+}$-PEI/CdTe QD bilayers (red curve).

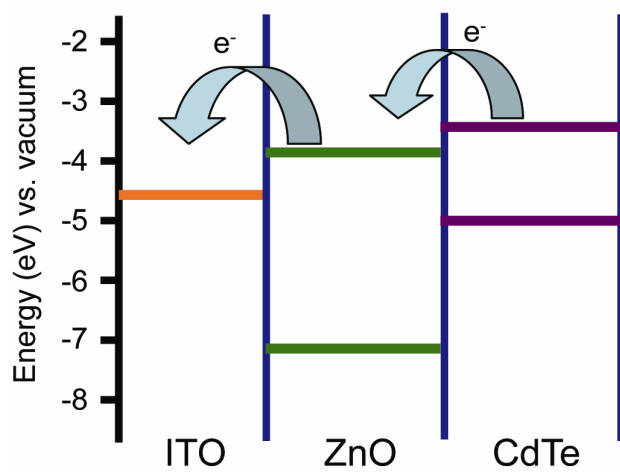**Figure S7.** Schematic diagram of charge transfer at the CdTe-ZnO interface.

Part 2. Photoelectrocatalytic performance of CdTe QD encapsulated ZnO nanorod arrays for phenol degradation

(a)

(b)
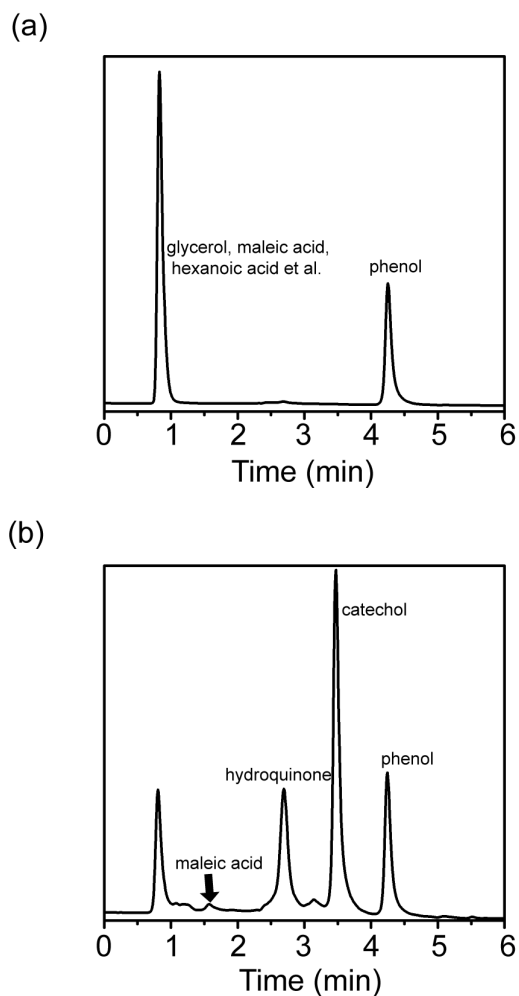
Figure S8. HPLC chromatogram of (a) photoelectrocatalytic degradation (reaction time: 2.5 h) and (b) photocatalytic degradation (reaction time: 5 h) of phenol using CdTe QD encapsulated ZnO nanorod arrays.
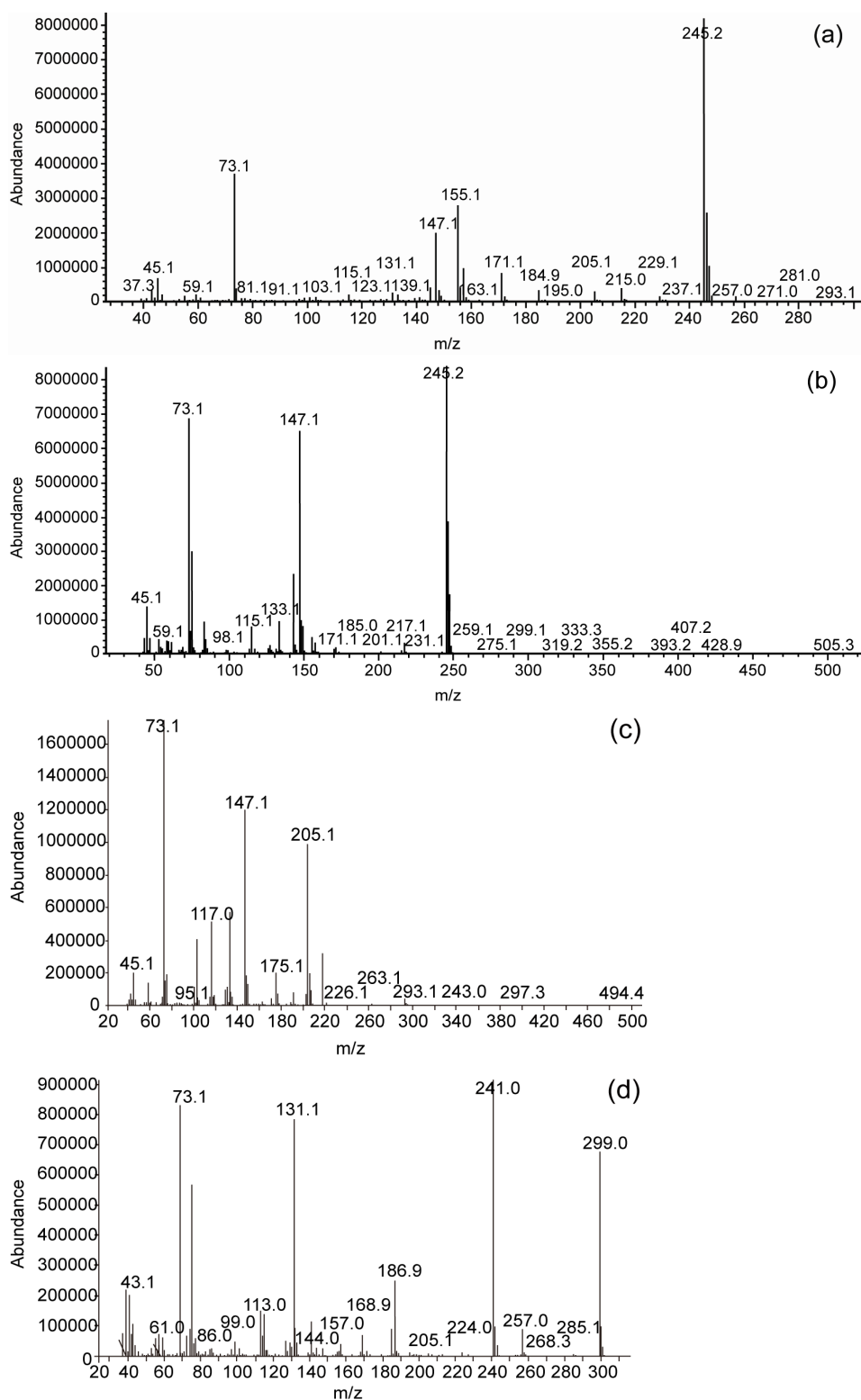
Figure S9. Mass spectrum of some products after derivatization by MSTFA and TMIS: (a) hydroxy-propyl acid, (b) maleic acid, (c) glycerol, and (d) hexanoic acid, resulting from phenol degradation by CdTe QD encapsulated ZnO nanorod arrays.
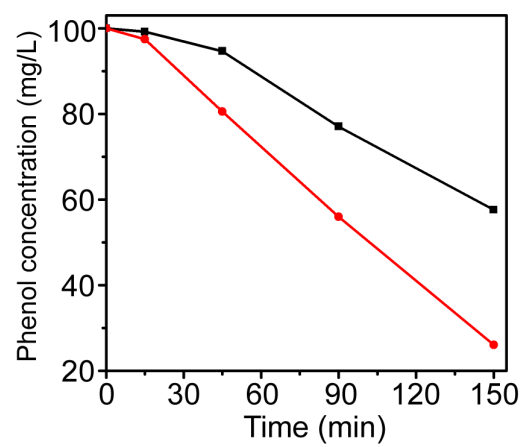
Figure S10. Phenol degradation in the photoelectrocatalytic process under oxygen (●) or nitrogen atmosphere (■).

Table S1 Comparison of removal efficiency of phenol by chemical oxidation, biological methods, photocatalytic degradation and electrochemically assisted photocatalysis.

Catalyst	Reaction conditions	Removal efficiency	TOC removal	Intermediates	Ref.
Fenton					
Fe^{2+} and H_2O_2	$[Fe^{2+}]_0=1$ mg/L, $[H_2O_2]_0=500$ mg/L, $pH_0=3$	Completely degraded within 4 h for 50 mL of 100 mg L^{-1} phenol solution	6% within 4 h	Catechol, hydroquinone, p-benzoquinone, oxalic acid, formic acid, maleic acid, et al.	S5
mesoporous Co_3O_4 /MnO_2 nanoparticles	Catalyst loading of 0.1 g/L, oxone loading = 0.5 g/L	Completely degraded within 100 min for 500 mL of 25 mg L^{-1} phenol solution	60-70% within 1.5h	4-hydroxybenzonic acid, 1,2-dihydroxybenzene, ρ-benzoquinone	S6
Biodegradation					
P. australis-strain IT-4 and *P. australis* plant	10^5 colony forming units (CFU) (g dry sediment)$^{-1}$, 28 ℃, 16:8 h light/dark	94.8% within 21 d for 100 mg [kg dry sediment]$^{-1}$ 4-*tert*-OP		2,2,4-trimethyl-1-penta nol, hydroquinone, 2-octylhydroquinone	S7
Coculture of PG-02 and PG-08	$2.0-2.3\times10^6$ colony forming units (CFU) mL^{-1}, 25 ℃	Completely degraded within 29 h for 100 mL of 250 mg L^{-1} phenol solution			S8
Photodegradation					
Pt/I-TiO_2	400 W dysprosium lamp, visible light, Catalyst loading of 1.0 g/L	62% within 2.5h for 1.5 L of 23.6 mg L^{-1} phenol solution	Ca. 38% within 2.5h	Quinone, oxalic acid, formic acid	S9
Cu_2O/TiO_2 nanosheets	$\lambda>420$ nm, Catalyst loading of 2.5 g/L	Ca. 77% within 2.5h for 40 mL of 10 mg L^{-1} phenol solution			S10
Electrochemically assisted photocatalysis					
Nanocrystalline TiO_2 electrode	130 mW/cm^2, +0.7 or 1.1 V, 9 cm^2		Ca. 40% within 2.5h for 10 mL of 100 mg L^{-1} phenol solution	Hydroquinone and benzoquinone	S11
p-SiNW/TiO_2 cathode	$\lambda>422$ nm, 94.5 mW/cm^2, -2.0 V (vs Ag/AgCl), 3 cm^2	80.7% within 100 min for 30 mL of 10 mg L^{-1} phenol solution	Up to 62% in 6 h	benzoquinone	S12
Bifunctionalized dye-sensitized	420 nm<λ< 500 nm, 4 mW/cm^2,	Ca. 90% within 2h for 14 mL of 10 mg		Hydroquinone and benzoquinone	S13

TiO$_2$ film	+0.5 V, 2 cm^2	L^{-1} phenol solution			
Bi$_2$WO$_6$ films with nanoleaflike structures	500-W Xe lamp, +0.6 V (vs SCE), 3.75 cm^2	about 78% in 3 h for 15 mL of 10 mg L^{-1} phenol solution	about 66% in 3 h		S14
CdTe Quantum Dots-encapsulated ZnO Nanorods	λ>400 nm, 130 mW/cm^2, +1.0 V (vs SCE), 4.15 cm^2	75% within 2.5h for 50 mL of 100 mg L^{-1} phenol solution	Up to 53.2% within 2.5h	hydroxy-propyl acid, glycerol, maleic acid and hexanoic acid	This study

Reference:

(S1) Li, X.; Zhou, Y.; Zheng, Z.; Yue, X.; Dai, Z.; Liu, S.; Tang, Z. Glucose Biosensor Based on Nanocomposite Films of CdTe Quantum Dots and Glucose Oxidase. *Langmuir* **2009**, *25*, 6580-6586.

(S2) Yu, W. W.; Wang, Y. A.; Peng, X. G. Formation and Stability of Size-, Shape-, and Structure-Controlled CdTe Nanocrystals: Ligand Effects on Monomers and Nanocrystal. *Chem. Mater.* **2003**, *15*, 4300-4308.

(S3) Peng, C.; Jiang, B.; Liu, Q.; Guo, Z.; Xu, Z.; Huang, Q.; Xu, H.; Tai, R.; Fan, C. Graphene-templated Formation of Two-dimensional Lepidocrocite Nanostructures for High-efficiency Catalytic Degradation of Phenols. *Energy Environ. Sci.* **2011**, *4*, 2035-2040.

(S4) Guo, Z. F.; Ma, R. X.; Li, G. J. Degradation of Phenol by Nanomaterial TiO$_2$ in Wastewater. *Chem. Eng. J.* **2006**, *119*, 55-59.

(S5) Zazo, J. A.; Casas, J. A.; Molina, C. B.; Quintanilla A.; Rodriguez, J. J. Evolution of Ecotoxicity upon Fenton's Oxidation of Phenol in Water. *Environ. Sci. Technol.* **2007**, *41*, 7164-7170.

(S6) Liang, H. W.; Sun, H. Q.; Patel, A.; Shukla, P.; Zhu, Z. H.; Wang, S. B. Excellent Performance of Mesoporous Co$_3$O$_4$/MnO$_2$ Nanoparticles in Heterogeneous Activation of Peroxymonosulfate for Phenol Degradation in Aqueous Solutions. *Appl. Catal. B: Environ.* **2012**, *127*, 330-335.

(S7) Toyama, T.; Murashita, M.; Kobayashi, K.; Kikuchi, S.; Sei, K.; Tanaka, Y.; Ike M.; Mori, K. Acceleration of Nonylphenol and 4-tert-Octylphenol Degradation in Sediment by *Phragmites australis* and Associated Rhizosphere Bacteria. *Environ. Sci. Technol.* **2011**, *45*, 6524-6530.

(S8) Jiang, H. L.; Tay, J. H.; Maszenan, A. M.; Tay, S. T. Enhanced Phenol Biodegradation and

Aerobic Granulation by Two Coaggregating Bacterial Strains. *Environ. Sci. Technol.* **2006**, *40*, 6137-6142.

(S9) He, Z. Q.; Xie, L.; Tu, J. J.; Song, S.; Liu, W. P.; Liu Z. W.; Fan, J. Q.; Chen, J. M. Visible Light-Induced Degradation of Phenol over Iodine-Doped Titanium Dioxide Modified with Platinum: Role of Platinum and the Reaction Mechanism. *J. Phys. Chem. C* **2010**, *114*, 526-532.

(S10) Liu, L. C.; Gu, X. R.; Sun, C. Z.; Li, H.; Deng, Y.; Gao, F.; Dong, L. In situ loading of ultra-small Cu_2O particles on TiO_2 nanosheets to enhance the visible-light photoactivity. *Nanoscale* **2012**, *4*, 6351-6359.

(S11) Oliveira, H. G.; Nery, D. C.; Longo, C. Effect of Applied Potential on Photocatalytic Phenol Degradation Using Nanocrystalline TiO_2 Electrodes. *Appl. Catal. B: Environ.* **2010**, *93*, 205-211.

(S12) Yu, H. T.; Li, X. Y.; Quan, X.; Chen, S.; Zhang, Y. B. Effective Utilization of Visible Light (Including $\lambda > 600$ nm) in Phenol Degradation with p-Silicon Nanowire/TiO_2 Core/Shell Heterojunction Array Cathode. *Environ. Sci. Technol.* **2009**, *43*, 7849-7855.

(S13) Qin, G. H.; Wu, Q. P.; Sun, Z.; Wang, Y.; Luo, J. Z.; Xue, S. Enhanced Photoelectrocatalytic Degradation of Phenols with Bifunctionalized Dye-sensitized TiO_2 film. *J. Hazard. Mater.* **2012**, *199-200*, 226-232.

(S14) Sun, S. M.; Wang, W. Z.; Zhang, L. Efficient Contaminant Removal by Bi_2WO_6 Films with Nanoleaflike Structures through a Photoelectrocatalytic Process. *J. Phys. Chem. C* **2012**, *116*, 19413-19418.